Recognition of *Aloe vera* compounds as potential inhibitors of SARS-CoV-2 NSP-16: Molecular docking approach for drug development

Abhinav Das [a], Divya Shaji [b *]

[a] Carmel Central School, Kerala - 680567, India

[b] Independent researcher, Kerala - 680642, India

Abstract

Severe Acute Respiratory Syndrome Corona Virus (SARS-CoV-2) is a rapidly spreading virus that appeared at the end of 2019 in Wuhan, China. To date, there is no effective treatment for COVID-19. *Aloe vera* is a widely used medicinal plant and its antiviral activities are well documented. A molecular docking approach was employed in this study to identify the drug lead compounds from *Aloe vera* against SARS-CoV-2 Non-Structural Protein 16 (NSP-16). A set of 14 *Aloe vera* compounds satisfying 'Lipinsky's rule of five' was collected from the literature. The results suggested that compounds feralolide, aloe-emodin, eupatorin, aloesaponarinII, chrysophanol and aloesaponarinI can bind strongly to the active site of NSP-16, and can be promising natural candidates to inhibit NSP-16.

Key words: SARS-CoV-2, aloe vera, NSP-16, docking, feralolide, aloe-emodin, eupatorin, COVID-19, methyl transferase, aloesaponarin, chrysophanol

1. Introduction

Corona virus disease (COVID-19) is an infectious disease caused by a newly discovered Severe Acute Respiratory Syndrome Corona Virus 2 (SARS-CoV-2). This virus spread rapidly all over the world, poses an increasing threat to human health. The World Health Organization (WHO) officially declared the COVID-19 as a pandemic on March 11, 2020 [1, 2]. At present, there is no effective antiviral drug or treatment for COVID-19. In this scenario, there is an emergent need for the most effective antiviral drugs. Although COVID-19 vaccines have been developed, the safety, efficacy, durability and availability to large population have not been established. Unfortunately, it is still unclear how long COVID-19 vaccines will provide protection [3].

Medicinal plants produce primary and secondary metabolites, provide a large number of integral and alternative medicines. Natural products from medicinal plants have been an important source of more efficient drugs [2,3,4]. Bioactive compounds extracted from various parts of these plants are responsible for the therapeutic effects of phyto-antivirals which include anthraquinones, coumarins, flavonoids, alkaloids etc. [4]. According to the World Health Organization (WHO), more than 80% of the population in Africa and over 65% of the world population uses herbal medicine to meet their primary health care needs [4, 5]. Herbal medicines are safe, effective, and have fewer side effects compared to allopathic medicines [5]. Recently, the role of herbal medicine in the treatment of COVID-19 has been reported [5, 6,7].

Aloe vera (Aloe barbadensis Miller) is the most common aloe variety, a perennial herb with 30–60 cm long juicy leaves, belonging to the family *Liliaceae,* native to the Mediterranean region, the Arabian Peninsula, India, China and Eastern Africa. Most bioactive compounds are contained in the leaves of *Aloe vera* that are filled with brown or yellowish milky juice [8, 9]. *Aloe vera* gel is usually used for therapeutic purposes. Traditonally, it has been used both externally and internally for the treatment of minor burns, wounds, skin irritations, cough, headaches, diabetes, ulcers etc. [10]. Apart from medicinal uses, *Aloe* gels have an vital role in food preservation as edible coatings. Recently, edible coatings have obtained more attention because of their potential for developing edible packaging materials [11]. Chromone and anthraquinone are the two-main class chemical constituents of the *Aloe vera* plant extract [11]. Antiviral properties of *aloe vera* on several types of viruses have already been reported in previous studies [5]. In addition to its antiviral properties, it has anti-inflammatory, anti-bacterial, anti-fungal, and immune-stimulant properties [5, 12].

Non-Structural Protein 16 (NSP-16), a viral RNA methyltransferase (Mtase), is one of the most promising drug target among corona viruses [13, 14]. In this study, we performed molecular docking with the compounds from *Aloe vera* and investigated the binding affinity of these compounds against SARS-CoV-2 NSP-16. We selected six lead compounds from *Aloe vera* that

may be suitable for further analysis as potential inhibitors of SARS-CoV-2 NSP-16. Interestingly, top scored compounds exhibited higher binding energies than that of the co-crystallized inhibitor sinefungin.

2. Materials and Methods

2.1. Protein preparation

Crystal structure of nsp10-nsp16 methyltransferase complex (PDB ID: 6YZ1) was retrieved from the Protein Data Bank (https://www.rcsb.org/) [15]. 6YZ1 is a heterodimer containing nsp10 and NSP-16 in a complex form [16]. In this study, we used a single chain of NSP-16 (chain A) for docking analysis. Water molecules and the co-crystallized ligand sinefungin were removed from the protein and hydrogen atoms were added. In addition, both the Kollman and gasteiger charges were added, saved in .pdbqt format using AutoDock Tools 1.5.7 [17].

2.2. Ligand preparation

14 compounds from various parts of *Aloe vera*, satisfying 'Lipinsky's rule of five' [18] were collected from the literature [5,9-12,19]. The 3D structures of selected ligands were retrieved in .sdf format from PubChem (https://pubchem.ncbi.nlm.nih.gov/) [20] and the structures were then converted into .pdb format using OpenBabel [21]. Gasteiger charges were added to the ligands using AutoDock Tools [17]. The co-crystallized ligand sinefungin was used as the reference. [16].

2.3. Drug likeness of the ligands

The physicochemical properties of the *Aloe vera* compounds according to 'Lipinsky's rule of five' [18] were calculated using SwissADME [22]. The SMILES of the selected compounds were taken from PubChem [20] and submitted to SwissADME [22].

2.4. Molecular Docking

AutoDock 4.2.6 [17] was used for molecular docking . The PDB files of both ligands and proteins were converted in to .pdbqt format using Autodocktools [17]. Grid spacing was set to 0.375Å (default). Center grid box values were set to x = 83.948, y = 15.107, and z = 28.137. The number of grid points along the x, y, and z dimensions was set as 36 x 36 x 36. The genetic algorithm was set as follows: i) the number of GA runs: 250; ii) population size: 150; iii) the number of energy evaluations: 2500000; and iv) the maximum number of generations: 27000. The Lamarckian genetic algorithm was used and the output was saved in docking parameter file (DPF) format.

2.5. Docking validation

For validating our docking procedure, the co-crystallized ligand was redocked in to the active site of target protein. Root-mean-square deviation (RMSD) between the co-crystallized and redocked complex was calculated [23]. RMSD was obtained from the .dlg file of AutoDock output [17].

3. Results and discussion

3.1 Molecular docking

Molecular docking is a powerful approach for investigating the binding interactions between the ligands and target proteins. It allows us to characterize the behavior of ligands in the active site of target proteins as well as to elucidate the fundamental biochemical processes. The process of molecular docking involves two steps (1) prediction of the ligand conformation as well as its position and orientation within these sites (usually referred to as 'Pose') and (2) assessment of the binding affinity. These two steps are related to sampling methods and scoring schemes, respectively [24].

In the present study, a set of 14 compounds were selected from *Aloe vera* to assess their potential against SARS-CoV-2 NSP-16. The chemical structures of the *aloe vera* compounds used for docking study are shown in Fig.1. The selected 14 compounds were obeying 'Lipinsky's rule of five' which is a rule of thumb to evaluate the drug-like-ness of a chemical compound. 'Lipinsky's rule of five' states that an orally active drug has (1) less than 5 hydrogen-bond donors, (2) less than 10 hydrogen-bond acceptors, (3) molecular mass less than 500 g/mol and (4) lipophilicity expressed as logP not greater than 5 [18]. In addition, the topological polar surface area (TPSA) and the number of rotatable bonds of the compounds were calculated. TPSA and the number of rotatable bonds should be less than 140 $Å^2$ and less than 10, respectively [25]. All the compounds in this study satisfied the above properties. The physicochemical properties of the compounds predicted by SwissADME [22] are shown in Table1.

The SARS-CoV-2 NSP-16 is an S-adenosyl-L-methionine (SAM)-dependent methyltransferase. 2′-O-RNA methyltransferase (MTase) is one of the enzymes of SARS-CoV-2 that is a promising target for antiviral therapy as it is necessary for RNA cap formation; a vital process for viral RNA stability. This MTase function is associated with the NSP-16 protein, which requires a cofactor, nsp10, for its proper activity [16]. SARS-CoV-2 NSP-16 shares 93.3% identity with SARS-CoV NSP-16. Genetic disruption of SARS-CoV NSP-16 leads to a ten-fold reduction in the formation of viral RNA. For this reason, NSP-16 is an attractive drug target for COVID-19 [26]. The methyl donor SAM plays a major role in the complex formation of NSP10-NSP16 and it increases RNA binding [13]. For stabilizing the SAM binding site, NSP-10 interacts with Nsp16 through hydrophobic and electrostatic interactions [26]. Small compounds may potentially inhibit methyltransferase activity of the SARS-CoV-2 NSP10-NSP16 complex by binding to the SAM-binding pocket [14]. Sinefungin, a pan-MTase inhibitor isolated from *Streptomyces griseoleus,* binds within the SAM-binding pocket [16].

In order to discover the potential natural inhibitors against SARS-CoV-2 NSP-16, we performed site-specific docking at the SAM-binding pocket using AutoDock4.2.6 [17]. Knowing the location of binding site before molecular docking, significantly enhances the efficiency of docking [24]. The native crystallized sinefungin was used as the reference standard for comparison. The structure of NSP-16 with its co-crystallized ligand sinefungin is shown in Fig.2. 250 poses were generated using an rmsd-tolerance of 2.0 Å for each aloe vera compound and a cluster having the larger number of poses was selected. After docking, the compounds were ranked according to their binding energy and the best lead compounds were selected based on the lowest binding energy (kcal/mol). The binding energies of the reference ligand and fourteen *aloe vera* compounds are shown in Table2. We compared the binding energies of the compounds with that of the co-crystallized ligand sinefungin. Small compounds binding with a greater binding energy compared to sinefungin may be potential methyltransferase inhibitors. The binding energy values of compounds range from –8.79 to –3.98 kcal/mol. Interestingly, compound feralolide exhibited the higher binding energy –8.79 kcal/mol, higher than that of the cocrystallized ligand sinefungin which showed only the binding energy –6.80 kcal/mol. Moreover, compounds aloe-emodin (–7.42 kcal/mol), eupatorin (–7.40 kcal/mol), aloesaponarin II (–7.31 kcal/mol), chrysophanol (–7.07 kcal/mol), aloesaponarin I (–7.02 kcal/mol) showed the higher binding energy than that of the native ligand. Binding energy of the co-crystallized ligand was placed in the seventh position, slightly lesser than that of aloesaponarin I. Binding energies of the compounds emodin (–6.52 kcal/mol) and anthranol (–6.42 kcal/mol) were somewhat close to that of the native inhibitor (–6.80 kcal/mol). The poorest ligand obtained in this study was salicylic acid which exhibited the binding energy –3.98 kcal/mol. Overall, binding energy values of *aloe vera* compounds indicate that six compounds (feralolide, aloe-emodin, eupatorin, aloesaponarinII, chrysophanol and aloesaponarinI) are the best promising ligands that can be used as potential inhibitors of the SARS-CoV-2 NSP-16.

3.2 Analysis of the docked complexes

The docked complexes between promising ligands and the receptor NSP-16 were analyzed by PyMol [27] and LigPlot [28]. Interestingly, all the fourteen compounds from *Aloe vera* formed hydrogen bonds with the amino acid residues of SARS-CoV-2 NSP-16. The amino acid residues of NSP-16 involved in hydrogen bonds and the number of hydrogen bonds for each *Aloe vera* compound along with the reference compound is shown in Table3. The reference compound sinefungin had five hydrogen bonds with the residues Asn43, Gly73, Asp99 and Asp130. Apart from this, hydrophobic interactions were also observed. Krafcikova et.al [16] reported that six residues Asn43, Asp99, Asn101, Asp114, Asp130, and Lys170 are highly conseved among SARS-CoV-2, SARS and MERS. Here, sinefungin formed the hydrogen bond interactions with three conserved residues Asn43, Asp99, and Asp130.

The best promising compound feralolide displayed four hydrogen bonds with the amino acids Gly71, Asn101, Cys115, Tyr132. Two dimensional and three dimesional representations of H-bonds and hydrophobic interactions of the feralolide-NSP-16 docked complex are shown in Fig 3A and 3B, respectively. Recently, Mpiana et.al conducted a docking study against Mpro with the ten *Aloe vera* compounds. The best scored compound in their study was feralolide with the binding energy −7.9 kcal/mol [1].

Aloe-emodin formed four hydrogen bonds with the residues Gly71, Asp99, Cys115 and Tyr132 (Fig 4A and 4B). Aloe-emodin is an anthraquinone compound, abundant in the leaves of *Aloe vera* [9]. Antiviral activities of aloe-emodin to some kind of viruses, such as SARS-CoV1, human herpes simplex virus type 1(HSV-1), HSV-2 and Varicella-Zoster virus (VZV) have been reported [5]. Antiviral activity of aloe-emodin against Influenza A virus has also been reported in a previous study [29].

Eupatorin made a hyrogen bond with the amino acid ASP130 which is a highly conseved residue among corona viruses (Fig 5A and 5B). Eupatorin is a flavonoid, usually found in a variety of fruits, vegetables and herbs. It is one of the strong candidates as anti-breast cancer agents. It has been reported that eupatorin suppresses proliferation and induces apoptosis in several cancer cell lines [30]. To the best of our knowledge, the antiviral activity of eupatorin has not been reported. However, here we showed that eupatorin could bind perfectly to the SAM-binding pocket of NSP-16, suggesting it as a potent inhibitor of SARS-CoV-2 NSP-16.

Aloesaponarin I and aloesaponarin II are the main anthraquinones of *Aloe vera* roots. Previous research pointed out the antiviral activity of aloesaponarin I and aloesaponarin II against influenza A virus [31]. Aloesaponarin I formed seven hydrogen bonds with the residues Asp75, Asp99, Leu100, Asn101,Asp130, Tyr132, Lys170 (Fig 8A and 8B) and aloesaponarin II formed three hydrogen bonds with the residues Asp99, Cys115 (Fig 6A and 6B). Interestingly, aloesaponarin I made hydrogen bond interactions with four highly conserved residues Asp99, Asn101, Asp130, and Lys170.

Chrysophanol, also known as chrysophanic acid is a natural anthraquinone. Chrysophanol formed three hydrogen bonds with the amino acids Asp99, Cys115, and Tyr132 (Fig 7A and 7B). Semple et.al found that chrysophanol inhibit the replication of poliovirus types 2 and 3 (Picornaviridae) in vitro. Chrysophanol is structurally similar to emodin and aloe-emodin, which are not active against poliovirus. They indicated that two hydrophobic positions on the chrysophanol (C-6 and the methyl group attached to C-3) were important for the compound's activity against poliovirus [32,33]. The effect of chrysophanol against Japanese encephalitis virus (JEV) was also reported in a previous study[34].

As shown in Table 3, caffeic acid formed hydrogen bonds with four conserved residues Asp99, Asn101, Asp130, and Lys170. Moreover, another compound uric acid formed hydrogen bonds with three conserved residues Asp99, Asp130, and Lys170. Interestingly, we observed that the residues Gly71, Cys115, and Tyr132 involved in hydrogen bond interactions with most of the *aloe-vera* compounds.

Based on the molecular docking study, Mpiana et. al. [1] reported that *Aloe vera* can be considered as a high potential plant against novel coronavirus SARS-CoV-2. Our study supports their hypothesis and proposes six drug lead compounds from *Aloe vera* for the management of COVID-19.

3.3 Docking validation

Validation of our docking study was carried out by redocking the native ligand in to the target protein. It was performed in order to measure the reliability of molecular docking. As shown in Fig.9, the re-docked complex was superimposed on to the co-crystallized complex using PyMOL [27]. Root-mean-square deviation (RMSD) between the re-docked complex and the co-crystallized complex was calculated [23, 35]. If the RMSD of re-docked conformation is less than 2.0 Å from the co-crystallized conformation, the prediction is said to be accurate. Our calculated RMSD is 1.6 Å which validated the success of our docking protocol.

Conclusion

In this study, the efforts have been made to discover potential SARS-CoV-2 NSP-16 inhibitors from the set of fourteen *Aloe vera* compounds using molecular docking. Our study identified six promising compounds based on the binding energy. The best lead compound is feralolide (–8.79 kcal/mol) followed by aloe-emodin (–7.42 kcal/mol), eupatorin (–7.40 kcal/mol), aloesaponarinII (–7.31 kcal/mol), chrysophanol (–7.07 kcal/mol) and aloesaponarinI (–7.02 kcal/mol). Interestingly, all these compounds showed higher binding energy than that of the co-crystallized ligand sinefungin (–6.80 kcal/mol). Based on the binding energy score, we suggest that these compounds can be tested for *in vitro* and *in vivo* investigations, to develop effective antiviral drugs for the treatment of COVID-19.

Conflict of interest:

The authors declare no conflict of interest.

Ethical approval:

This article does not contain any studies with human participants or animals performed by any of the authors.

References

1. Mpiana PT, Tshibangu DS, Kilembe JT, Gbolo BZ, Mwanangombo DT, Inkoto CL, Lengbiye EM, Mbadiko CM, Matondo A, Bongo GN, Tshilanda DD. Identification of potential inhibitors of SARS-CoV-2 main protease from Aloe vera compounds: A molecular docking study. Chem. Phys. Lett. 2020; 754:137751.

2. Narkhede RR, Pise AV, Cheke RS, Shinde SD. Recognition of natural products as potential inhibitors of COVID-19 main protease (Mpro): In-silico evidences. Nat. Prod. Bioprospecting. 2020; 10:297-306.

3. Abouelela ME, Assaf HK, Abdelhamid RA, Elkhyat ES, Sayed AM, Oszako T, Belbahri L, Zowalaty AE, Abdelkader MS. Identification of Potential SARS-CoV-2 Main Protease and Spike Protein Inhibitors from the Genus Aloe: An In Silico Study for Drug Development. Molecules. 2021;26:1767.

4. Lowe H, Steele B, Bryant J, Fouad E, Toyang N, Ngwa W. Antiviral Activity of Jamaican Medicinal Plants and Isolated Bioactive Compounds. Molecules. 2021;26:607.

5. Mpiana PT, Tshibangu DS, Kilembe JT, Gbolo BZ, Mwanangombo DT, Inkoto CL, Lengbiye EM, Mbadiko CM, Matondo A, Bongo GN, Tshilanda DD. Aloe vera (L.) Burm. F. as a potential anti-COVID-19 plant: a mini-review of its antiviral activity. European J Med Plants. 2020;24:86-93

6.Wang L, Wang Y, Ye D, Liu Q. Review of the 2019 novel coronavirus (SARS-CoV-2) based on current evidence. Int. J. Antimicrob. Agents. 2020;55:105948.

7. Malabadi RB, Meti NT, Chalannavar RK. Role of herbal medicine for controlling coronavirus (SARS-CoV-2) disease (COVID-19). International Journal of Research and Scientific Innovations. 2021;8:135-65.

8.Gansukh E, Gopal J, Paul D, Muthu M, Kim DH, Oh JW, Chun S. Ultrasound mediated accelerated Anti-influenza activity of Aloe vera. Sci. Rep. 2018;8:1-10.

9. Hęś M, Dziedzic K, Górecka D, Jędrusek-Golińska A, Gujska E. Aloe vera (L.) Webb.: natural sources of antioxidants–a review. Plant Foods Hum Nutr. 2019; 4:255-65.

10. Quispe C, Villalobos M, Bórquez J, Simirgiotis M. Chemical composition and antioxidant activity of Aloe vera from the Pica oasis (Tarapacá, Chile) by UHPLC-Q/Orbitrap/MS/MS. J. Chem. 2018;2018.

11. Kahramanoğlu İ, Chen C, Chen J, Wan C. Chemical constituents, antimicrobial activity, and food preservative characteristics of Aloe vera Gel. Agron. 2019;9:831.

12. Moghaddasi SM, Verma SK. Aloe vera their chemicals composition and applications: A review. Int J Biol Med Res. 2011;2:466-71.

13. Tazikeh-Lemeski E, Moradi S, Raoufi R, Shahlaei M, Janlou MA, Zolghadri S. Targeting SARS-COV-2 non-structural protein 16: a virtual drug repurposing study. J. Biomol. Struct. Dyn. 2020;1-4.

14. Liang J, Pitsillou E, Burbury L, Hung A, Karagiannis TC. In silico investigation of potential small molecule inhibitors of the SARS-CoV-2 nsp10-nsp16 methyltransferase complex. Chem. Phys. Lett. 2021;774:138618.

15. Berman HM, Westbrook J, Feng Z, Gilliland G, Bhat TN, Weissig H, Shindyalov IN, Bourne PE. The protein data bank. Nucleic Acids Res. 2000;28:235-42.

16. Krafcikova P, Silhan J, Nencka R, Boura E. Structural analysis of the SARS-CoV-2 methyltransferase complex involved in RNA cap creation bound to sinefungin. Nat.Commun. 2020;11:3717.

17. G.M. Morris, R. Huey, W. Lindstrom, et al., AutoDock4 and AutoDockTools4:automated docking with selective receptor flexibility, J. Comput. Chem. 2009;30:2785–2791.

18. C.A. Lipinski, Drug-like properties and the causes of poor solubility and poor permeability, J. Pharmacol. Toxicol. Methods. 2000;44:235–249.

19. Hamman JH. Composition and applications of Aloe vera leaf gel. Molecules. 2008 ;13:1599-616.

20. Kim S, Thiessen PA, Bolton EE, Chen J, Fu G, Gindulyte A, Han L, He J, He S, Shoemaker BA,Wang J. PubChem substance and compound databases. Nucleic Acids Res. 2015; 44:D1202-13.

21. O'Boyle NM, Banck M, James CA, Morley C, Vandermeersch T, Hutchison GR. Open Babel: An open chemical toolbox. J Cheminform. 2011; 3:33.

22. A. Daina, O. Michielin, V. Zoete, SwissADME: a free web tool to evaluatepharmacokinetics, drug-likeness and medicinal chemistry friendliness of smallmolecules, Sci. Rep. 2017; 7:42717.

23. Dhananjayan K. Molecular docking study characterization of rare flavonoids at the Nac-binding site of the first bromodomain of BRD4 (BRD4 BD1). J. Cancer Res. 2015;2015.

24. Meng XY, Zhang HX, Mezei M, Cui M. Molecular docking: a powerful approach for structure-based drug discovery. Curr. Comput.Aided Drug Des. 2011;7:146-57

25. D.F. Veber, S.R. Johnson, H.Y. Cheng, et al., Molecular properties that influence the oral bioavailability of drug candidates, J. Med. Chem. 2002;45:2615–2623.

26. Arya R, Kumari S, Pandey B, Mistry H, Bihani SC, Das A, Prashar V, Gupta GD, Panicker L, Kumar M. Structural insights into SARS-CoV-2 proteins. J. Mol. Biol. 2021;433:166725.

27. DeLano WL. Pymol: An open-source molecular graphics tool. CCP4 Newsletter on protein crystallography. 2002;40:82-92.

28. Wallace AC, Laskowski RA, Thornton JM. LIGPLOT: a program to generate schematic diagrams of protein-ligand interactions. Protein Eng Des Sel. 1995; 8:127-34.
29. Li SW, Yang TC, Lai CC, Huang SH, Liao JM, Wan L, Lin YJ, Lin CW. Antiviral activity of aloe-emodin against influenza A virus via galectin-3 up-regulation. Eur. J. Pharmacol. 2014; 738:125-32.
30. Abd Razak N, Abu N, Ho WY, Zamberi NR, Tan SW, Alitheen NB, Long K, Yeap SK. Cytotoxicity of eupatorin in MCF-7 and MDA-MB-231 human breast cancer cells via cell cycle arrest, anti-angiogenesis and induction of apoptosis. Sci. Rep. 2019;9:1-2.
31. Borges-Argáez R, Chan-Balan R, Cetina-Montejo L, Ayora-Talavera G, Sansores-Peraza P, Gómez-Carballo J, Cáceres-Farfán M. In vitro evaluation of anthraquinones from Aloe vera (Aloe barbadensis Miller) roots and several derivatives against strains of influenza virus. Ind Crops Prod. 2019;132:468-75.
32. Semple SJ, Pyke SM, Reynolds GD, Flower RL. In vitro antiviral activity of the anthraquinone chrysophanic acid against poliovirus. Antivir. Res. 2001;49:169-78.
33. Yusuf MA, Singh BN, Sudheer S, Kharwar RN, Siddiqui S, Abdel-Azeem AM, Fernandes Fraceto L, Dashora K, Gupta VK. Chrysophanol: a natural anthraquinone with multifaceted biotherapeutic potential. Biomolecules. 2019;9:68.
34. Chang, S.J.; Huang, S.H.; Lin, Y.J.; Tsou, Y.Y.; Lin, C.W. Antiviral activity of Rheum palmatum methanol extract and chrysophanol against Japanese encephalitis virus. Arch. Pharm. Res. 2014, 37, 1117–1123.
35. Tallei TE, Tumilaar SG, Niode NJ, Kepel BJ, Idroes R, Effendi Y, Sakib SA, Emran TB. Potential of plant bioactive compounds as SARS-CoV-2 main protease (Mpro) and spike (S) glycoprotein inhibitors: a molecular docking study. Scientifica. 2020;2020.

Table 1: Chemical properties of the 14 compounds contained in *Aloe vera*. Their PubChem ID, molecular weight (MW), number of rotatable bonds (RB), number of H-bond acceptors (HBA), number of H-bond donors (HBD), octanol-water partition coefficient (LogP), and total polar surface area (TPSA) calculated by SwissADME web tool [22].

	Compound	PubChem CID	MW(g/mol)	RB	HBA	HBD	LogP	TPSA (Å²)
1	anthranol	10731	194.23	0	1	1	3.41	20.23
2	chrysophanol	10208	254.24	0	4	2	2.38	74.60
3	emodin	3220	270.24	0	5	3	1.87	94.83
4	aloesaponarin II	3085033	254.24	0	4	2	2.08	74.60
5	aloe emodin	10207	270.24	1	5	3	1.50	94.83
6	aloesaponarin I	11098986	312.27	2	6	2	2.28	100.90
7	eupatorin	97214	344.32	4	7	2	2.53	98.36
8	feralolide	5317333	344.32	3	7	4	2.06	124.29
9	caffeic acid	689043	180.16	2	4	3	0.93	77.76
10	ferulic acid	445858	194.18	3	4	2	1.36	66.76
11	umbelliferone	5281426	162.14	0	3	1	1.51	50.44
12	esculetin	5281416	178.14	0	4	2	1.12	70.67
13	salicylic acid	338	138.12	1	3	2	1.24	57.53
14	uric acid	1175	168.11	0	3	4	-0.72	114.37

Table 2: Binding energy in kcal/mol for the fourteen *Aloe vera* compounds along with the reference compound sinefungin against NSP-16 of SARS-CoV-2.

	Compound	BE (kcal/mol)
	sinefungin (reference)	– 6.80
1	anthranol	– 6.42
2	chrysophanol	– 7.07
3	emodin	– 6.52
4	aloesaponarin II	– 7.31
5	aloe emodin	– 7.42
6	aloesaponarin I	– 7.02
7	eupatorin	– 7.40
8	feralolide	– 8.79
9	caffeic acid	– 5.13
10	ferulic acid	– 5.21
11	umbelliferone	– 6.29
12	esculetin	– 6.29
13	salicylic acid	– 3.98
14	uric acid	– 5.26

Table 3: Amino acids involved in H-bond interactions and the number of hydrogen bonds for each *aloe vera* compound against SARS-CoV-2 NSP-16.

	Compound	Residues involved in H-bonds	No: of H-bonds
	sinefungin (reference)	Asn43, Gly73, Asp99, Asp130	5
1	anthranol	Cys115	2
2	chrysophanol	Asp99, Cys115, Tyr132	3
3	emodin	Gly71, Cys115	2
4	aloesaponarin II	Asp99, Cys115	3
5	aloe emodin	Gly71, Asp99, Cys115, Tyr132	4
6	aloesaponarin I	Asp75, Asp99, Leu100, Asn101,Asp130, Tyr132, Lys170	7
7	eupatorin	Asp130	1
8	feralolide	Gly71, Asn101, Cys115, Tyr132	4
9	caffeic acid	Asp99, Leu100, Asn101, Asp130, Lys170	6
10	ferulic acid	Gly71, Ser98, Gly113, Tyr132	5
11	umbelliferone	Gly71, Tyr132	3
12	esculetin	Gly71, Tyr132	5
13	salicylic acid	Asp130	2
14	uric acid	Gly71, Gly73, Asp99, Asp130, Tyr132, Lys170	6

Figure 1: Chemical structures of the 14 compounds contained in *Aloe vera*

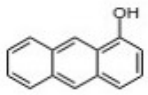

(1) Anthranol

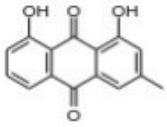

(2) Chrysophanol

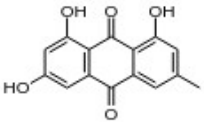

(3) Emodin

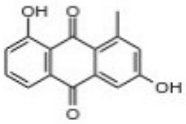

(4) Aloesaponarin II

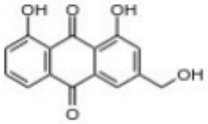

(5) Aloe-emodin

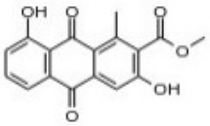

(6) Aloesaponarin I

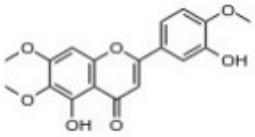

(7) Eupatorin

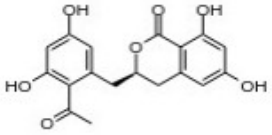

(8) Feralolide

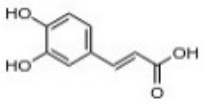

(9) Caffeic acid

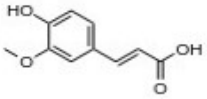

(10) Ferulic acid

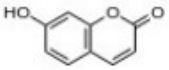

(11) Umbelliferone

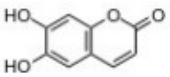

(12) Esculetin

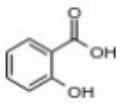

(13) Salicylic acid

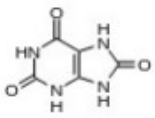

(14) Uric acid

Figure 2: Surface representation of SARS-CoV-2 NSP-16 with sinefungin (PDB ID: 6YZ1)

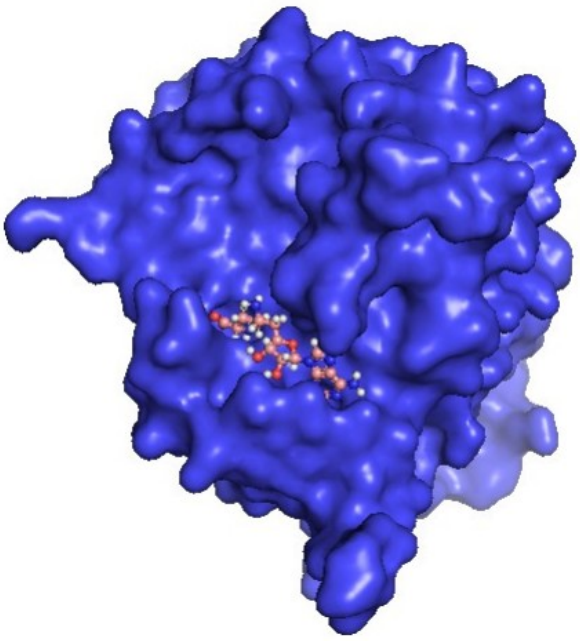

Figure 3. **(A)** Two dimensional representation of H-bonds and hydrophobic interactions of the best promising compound feralolide with SARS-CoV-2 NSP-16 using LigPlot [28]. H-bonds are displayed in green dotted lines. Residues involved in H-bonds and hydrophobic interactions are shown in green and blue colours, respectively. **(B)** Surface representation of NSP-16-feralolide docked complex.

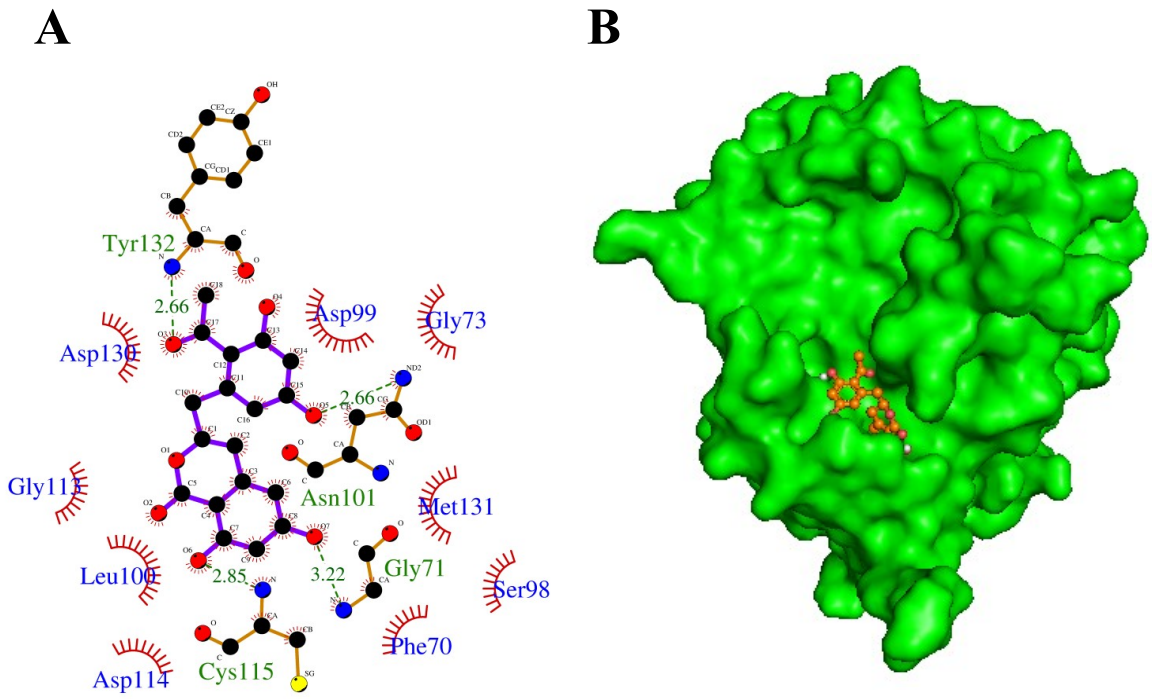

Figure 4. **(A)** Two dimensional representation of H-bonds and hydrophobic interactions of the second promising compound aloe-emodin with SARS-CoV-2 NSP-16 using LigPlot [28] . H-bonds are shown in green dotted lines. Residues involved in H-bonds and hydrophobic interactions are shown in green and blue colours, respectively. **(B)** Surface representation of NSP-16-aloe-emodin docked complex.

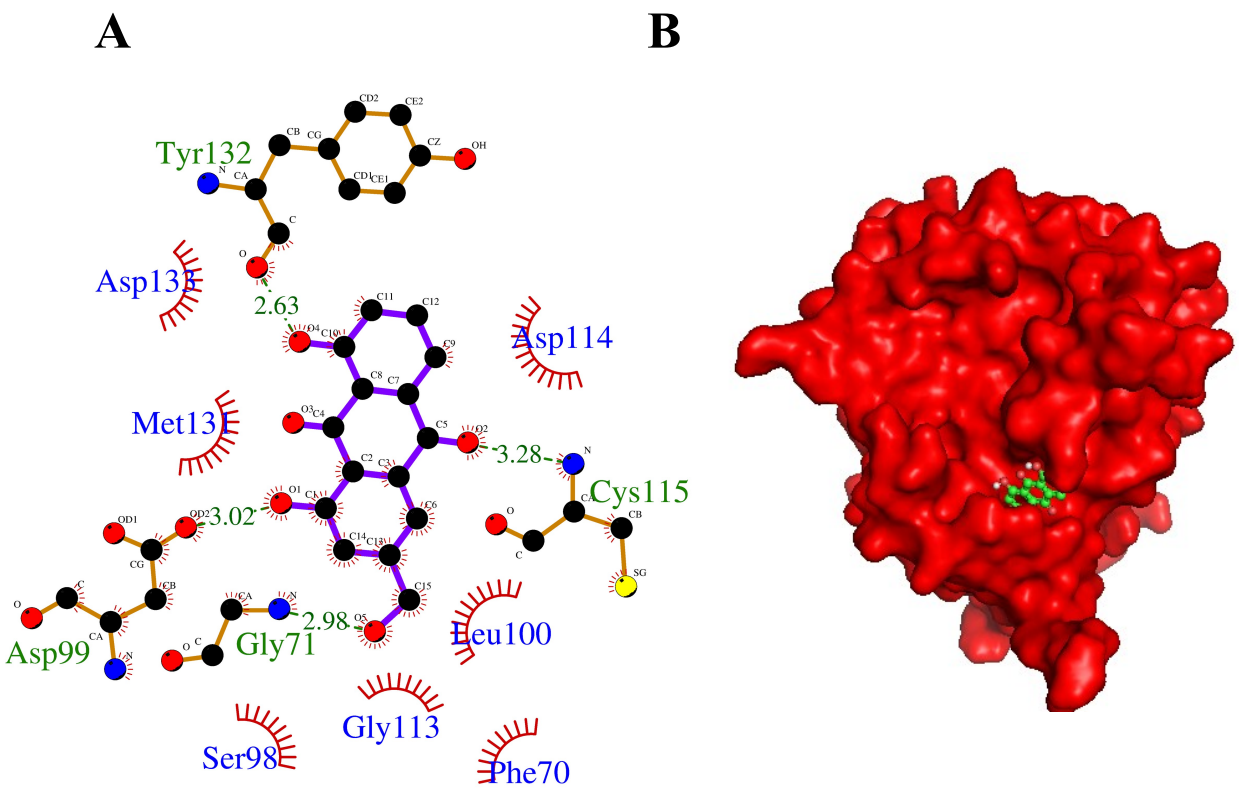

Figure 5. **(A)** Two dimensional representation of H-bonds and hydrophobic interactions of the third promising compound eupatorin with SARS-CoV-2 NSP-16 using LigPlot [28]. H-bonds are shown in green dotted lines. Residues involved in H-bonds and hydrophobic interactions are shown in green and blue colours, respectively. **(B)** Surface representation of NSP-16-eupatorin docked complex.

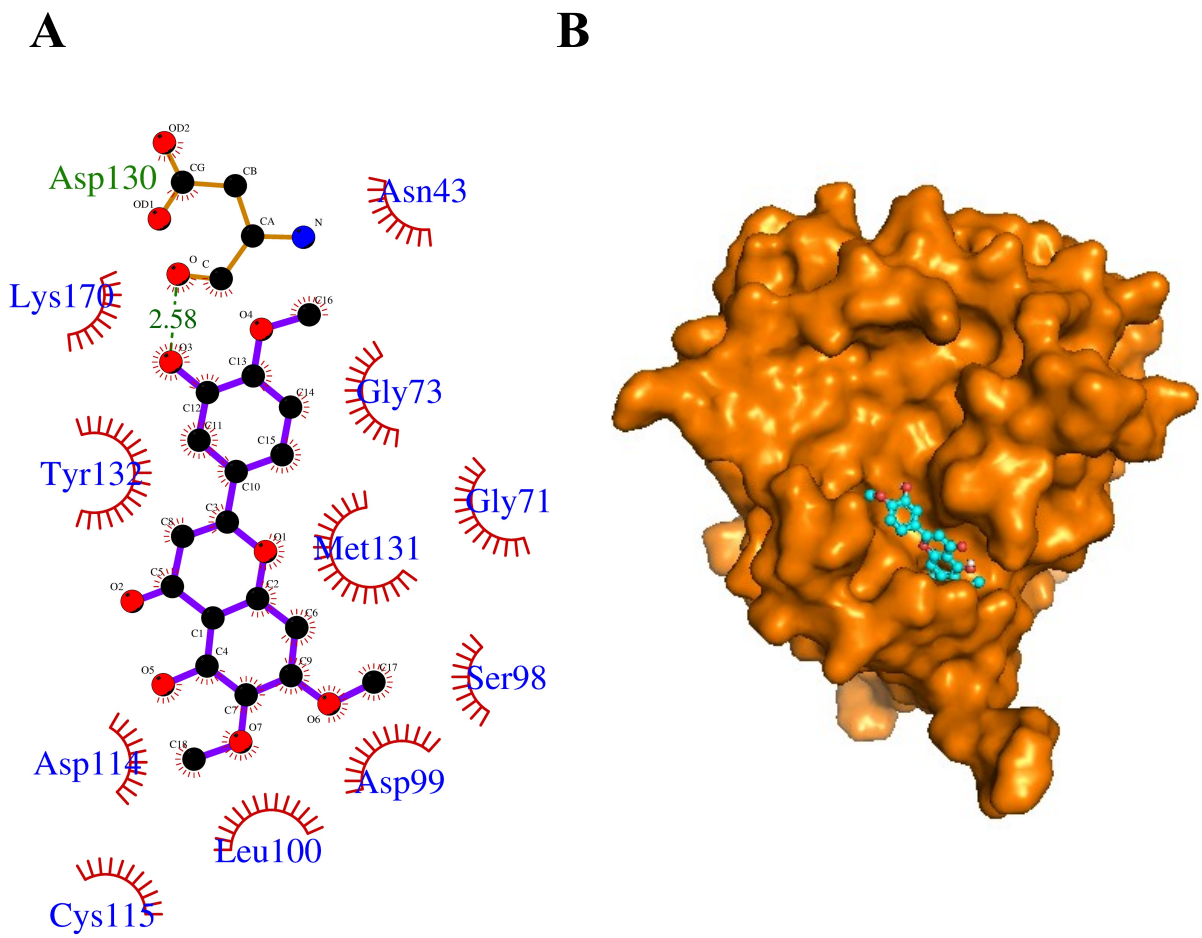

Figure 6. **(A)** Two dimensional representation of H-bonds and hydrophobic interactions of the fourth promising compound aloesaponarin II with SARS-CoV-2 NSP-16 using LigPlot [28]. H-bonds are shown in green dotted lines. Residues involved in H-bonds and hydrophobic interactions are shown in green and blue colours, respectively. **(B)** Surface representation of NSP-16-aloesaponarinII docked complex.

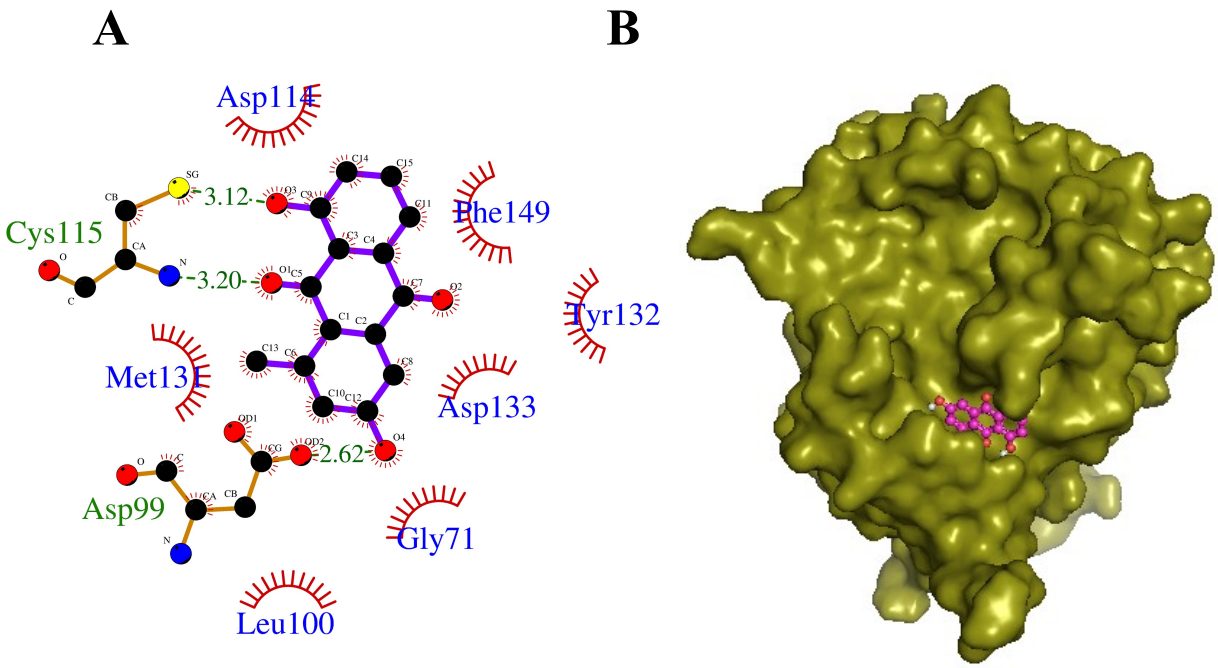

Figure 7. **(A)** Two dimensional representation of H-bonds and hydrophobic interactions of the fifth promising compound chrysophanol with SARS-CoV-2 NSP-16 using LigPlot [28]. H-bonds are shown in green dotted lines. Residues involved in H-bonds and hydrophobic interactions are shown in green and blue colours, respectively. **(B)** Surface representation of NSP-16-chrysophanol docked complex.

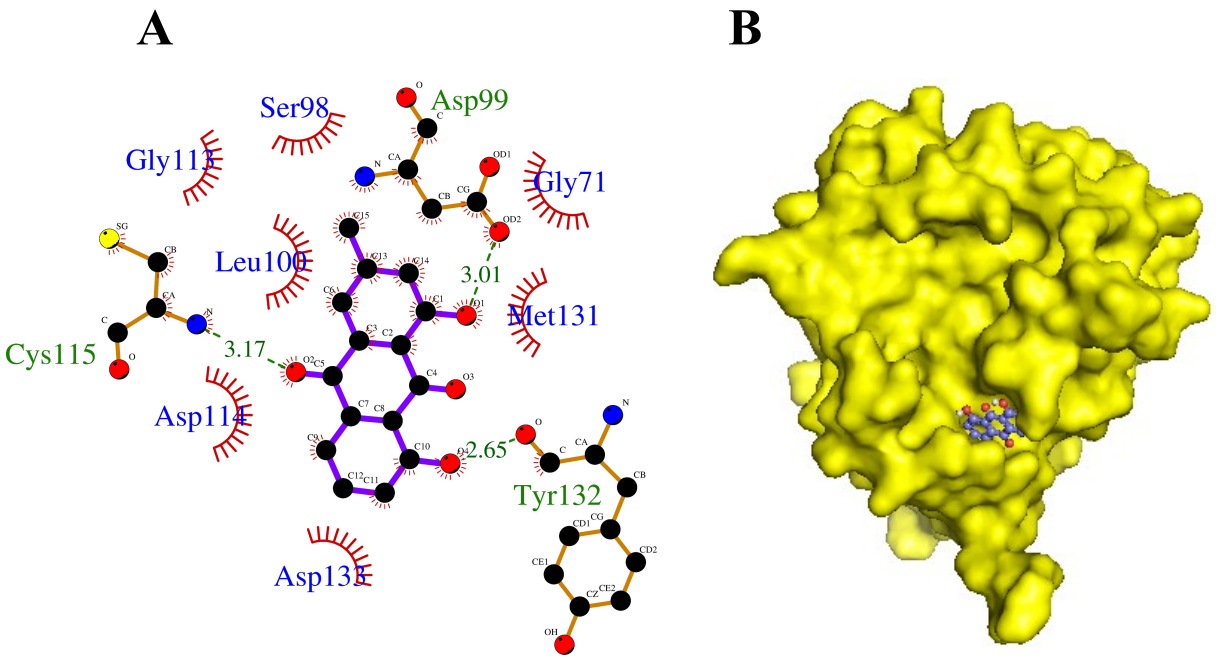

Figure 8. **(A)** Two dimensional representation of H-bonds and hydrophobic interactions of the sixth promising compound aloesaponarin I with SARS-CoV-2 NSP-16 using LigPlot [28]. H-bonds are shown in green dotted lines. Residues involved in H-bonds and hydrophobic interactions are shown in green and blue colours, respectively. **(B)** Surface representation of NSP-16-aloesaponarin I docked complex.

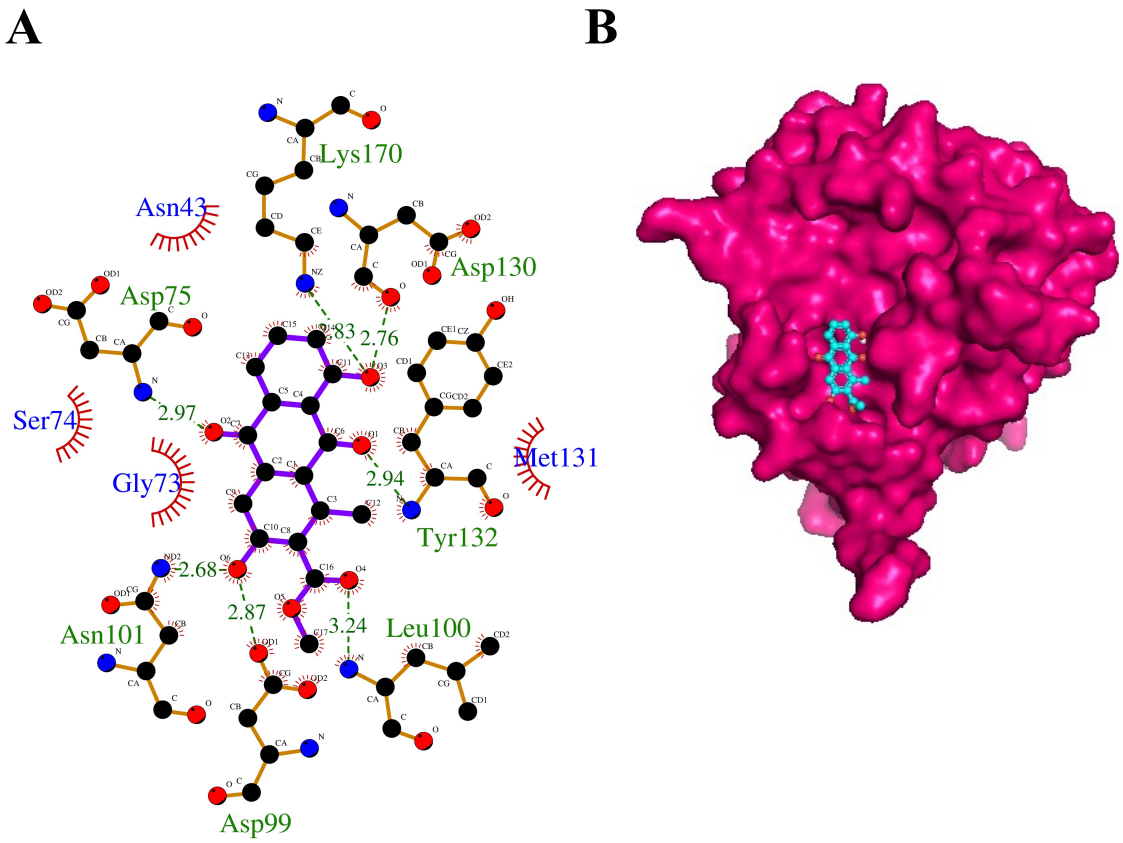

Figure 9. Validation of molecular docking. The red colour shows the co-crystallized pose retrieved from the crystal structure 6YZ1 and blue colour shows the re-docked pose of the ligand using AutoDock 4.2.6 [17].